Subnanoscale Characterization of MgO/Cu Heterophase Interfaces: Experiments and Atomistic Simulations

D. A. Shashkov, R. Benedek and D. N. Seidman

Department of Materials Science and Engineering and the Materials Research Center, Northwestern University, 2225 N. Campus Drive, Evanston, Illinois 60208-3108 USA

(Received: Mar. 12, 1997 Accepted: Mar. 17, 1997)

Abstract

Atomic-scale observations of {222}MgO/Cu and {222}MgO/Cu(Ag) ceramic/metal (C/M) interfaces by transmission electron (TEM), atom-probe field-ion (APFIM), and scanning transmission electron (STEM) microscopies, are complemented by *ab initio* atomistic modeling and molecular dynamics simulations. APFIM is employed to determine the identity of the terminating species at the interfaces and quantitatively analyze interfacial segregation of the solute (silver) species. Interfaces were synthesized by internal oxidation of binary or ternary copper-based alloys, which yields atomically clean C/M interfaces. Solute segregation was induced at C/M interfaces by annealing specimens with a ternary addition. The level of segregation, the Gibbsian interfacial excess, is directly determined by APFIM. *Ab initio* work-of-adhesion calculations are presented for polar {222}MgO/Cu coherent interfaces (zero-misfit approximation), based on local density functional theory (LDFT), and compared with experimental results. Adhesive energy calculations, as a function of interface spacing and translations parallel to the interface, are employed to devise an interatomic potential suitable for large-scale atomistic simulation. The interface structure, obtained with molecular dynamics (and statics) calculations based on the resultant potential, exhibits a misfit dislocation network with trigonal symmetry. The electronic spectra obtained with LDFT calculations show a localized interface state within the bulk MgO gap, at 0.5 eV below the Fermi energy.

1. Introduction

Ceramic/metal (C/M) interfaces have been a subject of considerable attention recently due to their presence in a wide range of materials and structures, including metal-matrix composites with ceramic fibers, metal/ceramic nanocomposites, machinable ceramics, electronic packaging, oxide scales on metals, and dispersion hardened alloys.[1,2] The adhesion of C/M interfaces has been a focus of much theoretical effort.[3,4,5,6,7] Recently, atomic-resolution observations of some well characterized C/M interfaces, such as Al_2O_3/Nb[1,2] and {100}MgO/Ag(100),[8] have been performed. {222}MgO/Cu interfaces have also been the subject of several recent experimental studies[9,10,11] as atomically clean C/M interfaces in this system, suitable for high-resolution electron microscopy (HREM) investigation, can be readily fabricated by internal oxidation. Alternatively, the focus of theoretical work has been mainly on nonpolar, electrically neutral C/M interfaces such as {100}MgO/Cu[12] and {100}MgO/Ag.[3,13,14,15]

This paper presents both experimental and simulation results on {222}MgO/Cu interfaces prepared by internal oxidation. In Section 2 we describe the experimental techniques for C/M interface fabrication and characterization. In Section 3 we present the results of an APFIM study of the chemistry of the terminating planes for the polar {222}MgO/Cu interface. In Section 4 APFIM measurements of segregation are detailed for Ag at {222}MgO/Cu interfaces. Section 5 summarizes our recent LDFT calculations for both polar C/M interfaces in the MgO/Cu system and their relation to the experimental APFIM results. Finally, Section 6 reviews the major conclusions of this paper.

2. Experimental Techniques

C/M interfaces for this study were prepared by internal oxidation. Advantages of this approach are: (1) clean interfaces with precisely controlled chemical composition; negligible impurity segregation – verified by APFIM – because of the large total interface area to volume ratio; (2) common low-index directions between the oxide precipitates and the matrix, with interplanar spacings suitable for HREM; (3) in fcc metals with a dispersion of rocksalt structure oxide precipitates, a simple cube-on-cube orientation often exists between the two phases. Precipitates are octahedral and are dominantly bounded by low-index {222} planes; and (4) the fiber axis of the Cu specimens is <111>, so that a random-area analysis, by APFIM, along this direction always

perpendicularly intersects a {222}C/M interface – see Fig. 1 for the geometry.
Atomically clean {222}MgO/Cu interfaces were formed by internally oxidizing a Cu-2.8 at.% Mg alloy for 0.5 h at 1173 K in a Rhines pack.[16] This procedure yields 5×10^{21} m^{-3} octahedral precipitates with a mean diameter of <20 nm, which are readily detectable by HREM and FIM. APFIM analysis also verified the purity of the matrix, with $<10^{-3}$ at.fr. O and $<10^{-3}$ at.fr. Mg after internal oxidation.

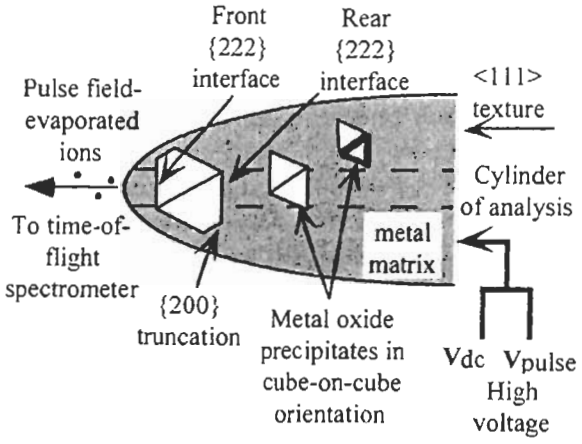

Fig. 1 Geometry of APFIM experiment used to analyze the atomic-scale chemistry of ceramic/metal interfaces. Note that due to the specimen texture, both "front" and "rear" interfaces are analyzed with maximum spatial resolution. The cylinder of analysis is determined by the size of the probe hole.

To study solute segregation at the same {222}MgO/Cu interface, we internally oxidized a single-phase ternary Cu(Mg,Ag) alloy fabricated from elements with high initial purity, thereby producing an atomically clean MgO phase embedded in a Cu(Ag) matrix. Interfaces were produced by internally oxidizing Cu-2.5 at.% Mg-1 at.% Ag alloy for 2 h at 1223 K using a Rhines pack. Octahedral-shaped MgO precipitates, 20–40 nm in diameter, were formed at a density of 10^{22} m^{-3}. To induce Ag segregation, specimens were annealed for 6 h at 773 K in an argon atmosphere.
Specimens containing atomically clean and segregated {222}MgO/Cu interfaces were prepared for APFIM and electron microscopy studies by electropolishing.[17] A scanning transmission electron microscopy (STEM) investigation was conducted on an ultrahigh resolution VG603 microscope at Oak Ridge National Laboratory. High-spatial resolution electron energy loss spectroscopy (EELS) and Z-contrast work was performed using a VG501 microscope at Cornell University.

3. Terminating Plane at a Polar {222}MgO/Cu Interface

The terminating ceramic layer at a polar C/M interface can be either cation or anion. In a recent investigation of a {222}MgO/Cu interface,[10] oxygen termination was suggested based on the analysis of HREM images.
In this study, APFIM analysis of the MgO/Cu system was performed along a <111> direction. In this case, the depth spatial resolution for chemical analysis is determined by the $d_{\{hkl\}}$ spacing of the $\{111\}_{metal}$ and $\{222\}_{metal\ oxide}$ planes. Thus, for the {222}MgO/Cu interface the resolution is 0.122 nm for MgO and 0.208 nm for Cu. For all interfaces observed the sequence of atoms across a {222}MgO/Cu interface is Cu|O|Mg|O|Mg|... and *not* Cu|Mg|O|Mg|O|..., which implies that the O termination is strongly preferred. This result is achieved without any deconvolution of the experimental data.[18]
In recent work, high-spatial resolution EELS was employed to observe the composition and electronic structure of {222}MgO/Cu interfaces.[19] EELS composition line scans across the interface unambiguously confirmed that the {222} interface is terminated by oxygen. The spatial resolution of that analysis is better than 1nm and is limited by beam broadening inside the specimen.
Finally, the first-principle calculations discussed in Section 5 also predict that O-terminated {222} interfaces are energetically preferred over Mg-terminated. Thus, oxygen termination of the {222}MgO/Cu interface is confirmed by three independent techniques.

4. Silver Segregation at a {222}MgO/Cu(Ag) Interface

APFIM analyses demonstrate strong segregation of Ag to the {222}MgO/Cu interfaces in this system. Figure 2 is an integral profile representing a complete dissection of a single MgO precipitate. Note the pronounced increase in Ag signal associated with both "front" and "rear" interfaces. To calculate Γ_{Ag} (the Gibbsian interfacial excess of Ag at a {222}MgO/Cu interface) the excess number of Ag atoms associated with an interface is normalized to the area of analysis. The former

is simply the height of the step in a Ag profile (Fig. 2), while the latter is obtained from geometrical considerations.[17]

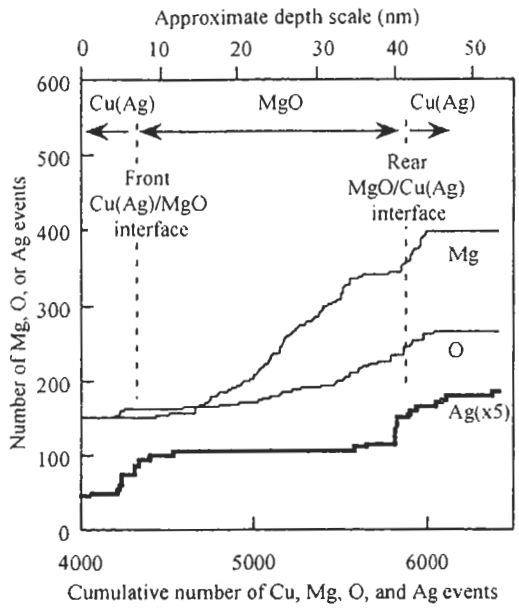

Fig. 2 APFIM integral profile through a single MgO precipitate embedded in a Cu(Ag) matrix after internal oxidation at 1223 K for 2 h and annealing at 773 K for 6 h. Note the sharp increase in the Ag signal at both front and rear interfaces, which demonstrates silver segregation at polar {222}MgO/Cu interfaces.

This analysis yields $\Gamma_{Ag} = (2\pm0.6)\times10^{15}$ atoms cm^{-2} at 773 K. APFIM analyses of 56,000 matrix atoms also demonstrates that the concentration is (0.47±0.03) at.% Ag in the Cu(Ag) matrix. Assuming segregation obeys a Langmuir-McLean isotherm, the *effective* Gibbs free energy of segregation of Ag to this {222}MgO/Cu(Ag) interface is 15.4 kJ mol^{-1} (or 0.16 eV $atom^{-1}$) at 773 K. The microscopic interpretation of this quantity is not straightforward, since MC simulations of grain boundary segregation demonstrate that different interface sites have different free energies of segregation[20] and solute-solute interactions are nonnegligible at this coverage. Therefore, this number represents an effective average over a spectrum of segregation sites with different free energies of segregation. Nevertheless the number is in the range commonly found (tenths of an eV) for solute segregation energies to interfaces and free surfaces.

Recently, we also studied silver segregation at {222}MgO/Cu interfaces using a dedicated STEM.[21] It was found that similar to atomically clean interfaces in this system, segregated interfaces are invariably terminated by oxygen. In addition, extra intensity was detected at the interfaces by Z-contrast microscopy, which is consistent with our APFIM results on silver segregation.

5. Atomistic Simulation of {222}MgO/Cu Interfaces

Atomistic simulations are essential to fully interpret the state-of-the-art atomic resolution probes (APFIM, high resolution and Z-contrast TEM, and EELS) that we are applying to the {222}MgO/Cu heterophase interface. Owing to the lack of accurate yet tractable interface interatomic-potential models, however, little progress has been made on simulating the atomic structure of ceramic-metal interfaces[22] and particularly the consequences of misfit. In recent work,[23] an approach that combines local-density functional theory (LDFT) calculations with classical simulations is applied to the MgO/Cu interface. LDFT calculations,[24] based on the coherent interface approximation, suggest that the most strongly bonded MgO/Cu interface is the oxygen-terminated {222} orientation, a result consistent with APFIM observations.[18] The relatively large misfit of {222}MgO/Cu (≈15%) must be accounted for in a realistic treatment of atomic structure. It cannot presently be included directly in the LDFT calculations, however, which scale rapidly with the size of the computational unit cell. Our strategy is to employ LDFT calculations to provide guidance as to an appropriate form of interatomic potential, suitable for classical simulation. Applying this potential in molecular dynamics and statics calculations, we predict a misfit dislocation network of trigonal symmetry.

5.1. Interface Potential Derived from LDFT Calculations

A familiar property related to interface bonding is the adhesive energy curve,[14] basically the total energy vs. interface spacing. The adhesive energy curve has been calculated by *ab initio* LDFT for a number of different (mostly nonpolar) interfaces of MgO or corundum with various metals. In general, the results follow reasonably closely the universal binding energy curve.[14] We note that all existing adhesive energy curve calculations approximate the interface as coherent, and thus neglect the misfit that exists for all real ceramic/metal

interfaces.

To gain insight into interface bonding for {222}MgO/Cu, we have calculated a family of adhesive energy curves, corresponding to different parallel translations of the coherent Cu interface layer, relative to the oxygen interface layer. The calculations are based on the plane-wave-pseudopotential representation of LDFT.[24] The most favorable registry for a coherent {222}MgO/Cu interfaces occurs for interface Cu atoms equidistant from three interface O atoms (the "hollow" position). For small parallel displacements from the hollow position, the adhesive energy curves deviate only slightly from the one previously determined. When the Cu atoms lie close to the "on top" positions directly above the oxygen atoms, however, the energy is considerably higher than the equilibrium curve for interface spacings in the vicinity of the equilibrium interface separation. To summarize, except for configurations close to the on-top positions, the adhesive energy depends essentially only on the interface separation, and not on translations parallel to the interface. It turns out that this behavior can be fitted very well in terms of a superposition of one and two-body analytical potentials. The one-body potential is the sum of Cu atoms at a distance z_i from the ceramic interface, which is assumed to be perfect and flat. The two-body potential is a Born-Mayer repulsive interaction between pairs of Cu and oxygen atoms at the interface.

5.2. Structure Simulations for {222}MgO/Cu

Employing this analytical interface potential we can now outline our molecular dynamics calculations for the {222}MgO/Cu polar interface. The MgO coordinates are frozen in their perfect-crystal configuration. A Cu EAM potential,[25] a computationally convenient analytical form, was employed. We treat a computational unit cell with 7 Cu and 6 O atoms per side (49 Cu and 36 O atoms per layer) and 12 Cu layers; as a control, we have performed another calculation with everything identical, except that the Cu interface layer has 6 atoms on a side and is therefore coherent with the oxygen. Larger computational cells will be used in future work. The atoms were started in perfect crystal positions and relaxed by a local optimization method, which is appropriate since no barriers exist to forming a dislocation network in this geometry.[26]

Figure 3 shows the relaxed atomic positions in the Cu interface layer projected onto a plane parallel to the interface (filled circles); the less densely packed O interface layer is represented by open circles. The simulated interface structure (which corresponds to T = 0 K) may be seen to exhibit an interfacial dislocation network of trigonal symmetry, consisting of dissociated partial dislocations lying along (1/2)<110> directions with a (1/6)<112> Burgers vector. Each unit cell of the trigonal network consists of two triangles, one of which corresponds to fcc and the other to hcp stacking at the interface.

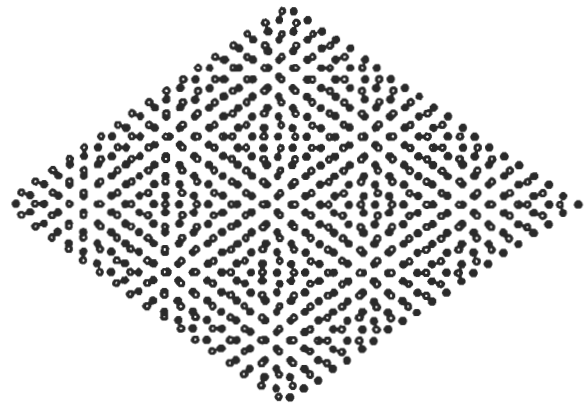

Fig. 3 Relaxed interface layer atomic positions projected onto the plane of the interface for Cu (filled circles) and O (open circles) calculated for oxygen-terminated {222} MgO/Cu interface.

The other geometrically possible interfacial structure is an hexagonal network of perfect dislocations lying along <112> directions with (1/2)<110> Burgers vectors. Incidentally, analogous dislocation networks were observed in simulations[27] based on *ad hoc* interatomic potentials designed to have the correct periodicity of {222}MgO/Cu interfaces, but otherwise not based on a detailed model of the bonding. Our calculations also show distortion of the layers normal to the interface, with interface Cu atoms near the on-top configuration displaced up to 0.2 Å away from the mean layer position. These distortions propagate out to the third layer, but essentially disappear by the fourth layer.

In principle, the trigonal and hexagonal networks are distinguishable by HREM,[9,27] but it has proven difficult, so far, to make a definitive identification on the basis of experiment alone. A recent Z-contrast microscopy investigation[21] was performed on a

{222}MgO/Cu interfaces with Ag segregation. The present simulation approach is being generalized to enable treatment of segregated Ag solute, and comparison with these experiments.

5.3. Interface Electronic Structure

In spite of the large misfit at the {222}MgO/Cu interface, coherent patches cover much of the interface area, and therefore electronic structure calculations based on the coherent interface approximation are expected to yield useful insights into the true interface. Layer-integrated density of electronic states calculations were performed in the vicinity of the oxygen-terminated {222}MgO/Cu interface within the coherent interface approximation (Fig. 4).

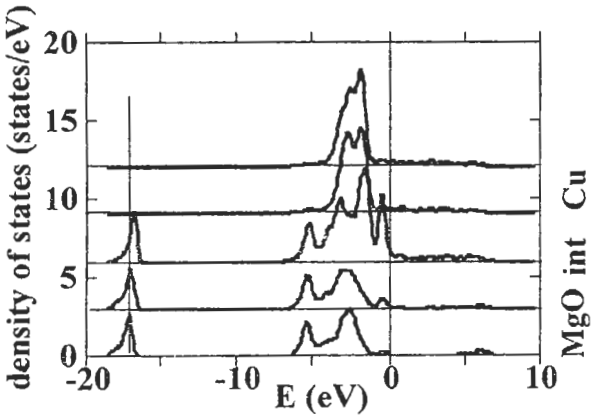

Fig. 4 Electronic density of states in vicinity of {222}MgO/Cu interface. The separate curves are obtained by integrating over slabs parallel to the interface. The curve labeled "int" superposes the Cu and the O layers at the interface. Also shown are results for the two adjacent layers on either side of the interface. Mg and O sublayers are combined, except at the interface.

These calculations utilized a multilayer geometry with 5 Mg layers, 6 O layers and 6 Cu layers per unit cell; the unit cell thus has two identical oxygen-terminated MgO/Cu interfaces. The local density of states is integrated over slabs centered on each of the layers; the Cu and O layers at the interface were combined, however. The energy zero corresponds to the Fermi energy. Except for the layers adjoining the interface itself, the layers on both sides of the interface show relatively bulk-like behavior. The peak at –17 eV on the MgO side corresponds to the O 2s band. This peak is slightly shifted to higher energy at the interface, which reflects an electrostatic potential shift. We note that the Cu d-band edge appears a few tenths of an eV higher than in bulk Cu calculations, as a result of the expansion of Cu to achieve coherence with MgO. A significant feature at the interface is a peak in the density of states at about 0.5 eV below the Fermi energy, within the MgO energy gap. This peak appears to represent an interface state (or "metal-induced gap state"[22]) that decays exponentially into the MgO. It is most likely a hybrid of Cu (4s) and O(2p) states. The perturbation of the electronic states at the {222}MgO/Cu interface has been recently observed by EELS.[21] Work is currently in progress to relate these EELS results to the LDFT calculations presented here.

6. Summary and Conclusions

Atom probe microscopy is used to determine the terminating layer at polar {222}MgO/Cu interfaces with a spatial resolution of 0.122 nm for MgO and 0.208 nm for Cu. The sequence of atoms observed across a {222}MgO/Cu interface is Cu|O|Mg|O|Mg|... which implies that O termination is at least strongly preferred. This result is confirmed by high-resolution EELS.

Quantitative measurements are presented of Ag segregation at {222}MgO/Cu interface. It is shown that the data are readily analyzed to obtain the Gibbsian interfacial excess of solute, and an *effective* Gibbs free energy of segregation.

Atomistic simulations of "coherent" C/M interfaces are performed based on LDFT within the plane-wave pseudopotential framework and *ab initio* work-of-adhesion, W, calculations are presented for polar MgO/Cu interfaces. The calculations demonstrate that O-terminated {222} interfaces have the largest W, and hence are favored in agreement with experiment.

We have developed a short-range interatomic potential model for the interface interaction, guided by *ab initio* LDFT calculations. Based on the model, we predict a misfit dislocation network of trigonal symmetry. Our electronic structure calculations exhibit an interface state at a binding of 0.5 eV.

This research was supported at Northwestern University by the U. S. Department of Energy, Office of Basic Energy Sciences, under grant DEFG02-96ER45597. Most of the numerical calculations were performed at the National Energy Research Supercomputer Center.

References

1. *Metal-Ceramic Interfaces: Proceedings of an International Workshop*, edited by M. Rühle, A. G. Evans, M. F. Ashby and J. P. Hirth (Pergamon Press, 1990).
2. *Proceedings of the International Symposium Metal/Ceramic Interfaces*, edited by W. Mader and M. Rühle, Acta Metall. Mater. **40**, supplement (1992).
3. D. M. Duffy, J. H. Harding, and A. M. Stoneham, Acta Metall. Mater. **43**, 1559 (1995).
4. C. Kruse *et al.*, J. Am. Ceram. Soc. 77, 431 (1994); Carsten Kruse, Dr. rer. nat., Universität Stuttgart, 1994.
5. F. Rao, R. Wu, and A. J. Freeman, Phys. Rev. B **51**, 10052 (1995).
6. P. Alemany *et al.*, J.Phys. Chem. **97**, 8464 (1995).
7. J. Purton, S. C. Parker, and D. W. Bullett, preprint (1996).
8. A. Trampert *et al.*, Acta Metall. Mater. **40**, S227 (1992).
9. W. P. Vellinga and J. Th. M. De Hosson, Materials Science Forum **207-209**, 361 (1996).
10. F. R. Chen *et al.*, Ultramicroscopy **54**, 179 (1994).
11. P. Lu and F. Cosandey, Ultramicroscopy **40**, 271 (1992).
12. Y. Li, D. C. Langreth, and M. R. Pederson, Phys. Rev. B **52**, 6067 (1995).
13. C. Li, A. J. Freeman, and C. L. Fu, Phys Rev B **48**, 8317 (1993).
14. T. Hong, J. R. Smith, and D. J. Srolovitz, Acta Metall. **43**, 2721 (1995); T. Hong, J. R. Smith, and D. J. Srolovitz, J. Adhes. Sci. Technol. **8**, 837 (1994).
15. U. Schönberger, O. K. Andersen, and M. Methfessel, Acta Metall. Mater. **40**, 1 (1992).
16. F. N. Rhines, Trans. AIME **137**, 246 (1940); F. N. Rhines, W. A. Johnson, and W. A. Anderson, Trans. AIME **147**, 205 (1942).
17. D. A. Shashkov and D. N. Seidman, Phys. Rev. Lett. **75**, 268 (1995); Appl. Surf. Sci. **94/95**, 416 (1996).
18. H. Jang, D. N. Seidman, and K. L. Merkle, Interface Science **1**, 61 (1993).
19. D. Muller *et al.*, in preparation for publication (1997).
20. J. D. Rittner, D. Udler, D. N. Seidman, and Y. Oh, Phys. Rev. Lett. **74**, 1115 (1995); J. D. Rittner, D. Udler, D. N. Seidman, Interface Science **4**, 65 (1996); J. D. Rittner, Ph.D. thesis, Northwestern University, 1996.
21. D. A. Shashkov *et al.*, in preparation (1997); D. A. Shashkov, Ph.D. thesis, Northwestern University (1997).
22. M. W. Finnis, *J. Phys.: Condens. Matter* **8**, 5811 (1996).
23. R. Benedek *et al.*, in preparation for publication (1997).
24. R. Benedek, M. Minkoff, and L. Yang, *Phys. Rev.* B **54**, 7697 (1996).
25. R. A. Johnson, *Phys. Rev.* B **37**, 3924 (1988).
26. C. M. Gilmore, *Phys. Rev.* B **40**, 6402 (1989).
27. W. P. Vellinga, Ph.D. thesis, University of Groningen, 1996.